Factoring of the Hyperfine Shifts in the Cyanide Adduct of Lignin Peroxidase from *P. chrysosporium*

Lucia Banci,[†] Ivano Bertini,*[,†] Roberta Pierattelli,[†] Ming Tien,[‡] and Alejandro J. Vila[§]

Contribution from the Department of Chemistry, University of Florence, Via Gino Capponi 7, 50121 Florence, Italy, The Pennsylvania State University, University Park, Pennsylvania 16802, and Departamento Quimica Biologica, Facultad de Ciencias Bioquimicas y Farmaceuticas, Universidad Nacional de Rosario, Suipacha 531, 2000 Rosario, Argentina

Received March 22, 1995[⊗]

Abstract: We have used NMR spectroscopy to study the cyanide derivative of lignin peroxidase with the goal of characterizing the electronic structure of this derivative of peroxidases. By using various homonuclear and heteronuclear 2D NMR techniques and by making use of the available X-ray structure of the cyanide-free protein, it has been possible to extend the assignment of the heme substituents and of the protons of some active-site residues. An estimate of the anisotropy and direction of the magnetic susceptibility anisotropy tensor has been obtained from the pseudocontact shifts of protons of residues not directly bound to the heme iron ion. Finally, a factoring of the hyperfine shifts of the heme and proximal histidine protons, as well as of the ^{13}C heme methyls and ^{15}N of the cyanide moiety, is obtained. The contact shift pattern of the heme protons is related to the orientation of the histidine plane. Very large upfield contact shifts are experienced by the aromatic protons of the proximal histidine. The axial magnetic anisotropy is smaller than in metmyoglobin–CN and slightly larger than in horseradish peroxidase–CN. This may reflect the order of the donor strength of the proximal histidine. The z axis of the magnetic susceptibility tensor is found essentially perpendicular to the heme plane.

Introduction

Knowledge of the electronic and magnetic properties of the metal ion in metalloenzymes can shed light on properties like the reduction potential of the metal ion and the mechanism of the enzymatic action. In this respect, the determination of the anisotropy of the magnetic susceptibility tensor through NMR investigations is a precious piece of information. This approach has been extensively applied to heme proteins.[1-8] Indeed, the factoring of the contributions to the NMR hyperfine shifts of the ^1H and ^{13}C nuclei of the heme and of the iron ligand(s) allows structural properties (such as the orientation and the tilt of the axial ligands), electronic properties (like the d orbital splitting), and the orientation of the magnetic susceptibility tensor to be correlated. This information can be further correlated with the reduction potential of the Fe^{3+}/Fe^{2+} and Fe^{4+}/Fe^{3+} pairs.

Peroxidases are heme proteins which catalyze the oxidation of a large number of substrates by hydrogen peroxide.[9-13] All heme–protein peroxidases share a common mechanism where active-site residues are highly conserved.[14] The study of lignin peroxidase (LiP) is of interest due to its high redox potential with respect to horseradish peroxidase (HRP) and cytochrome *c* peroxidase (CcP).[15-18] ^1H NMR studies on the cyanide derivative of LiP[19-22] have shown similarities among HRP,[23-25] CcP,[26-29] and LiP. This comparison has recently been extended to manganese peroxidase (MnP).[30] The X-ray structure of CcP

[†] University of Florence.
[‡] The Pennsylvania State University.
[§] Universidad Nacional de Rosario.
[⊗] Abstract published in *Advance ACS Abstracts*, July 15, 1995.

(1) Keller, R. M.; Wüthrich, K. *Biochim. Biophys. Acta* **1972**, *285*, 326–336.
(2) Williams, G.; Clayden, N. J.; Moore, G. R.; Williams, R. J. P. *J. Mol. Biol.* **1985**, *183*, 447–460.
(3) Emerson, S. D.; La Mar, G. N. *Biochemistry* **1990**, *29*, 1556–1566.
(4) Feng, Y.; Roder, H.; Englander, S. W. *Biochemistry* **1990**, *29*, 3494–3504.
(5) Gao, Y.; Boyd, J.; Pielak, G. J.; Williams, R. J. P. *Biochemistry* **1991**, *30*, 1928–1934.
(6) Rajarathnam, K.; La Mar, G. N.; Chiu, M. L.; Sligar, S. G. *J. Am. Chem. Soc.* **1992**, *114*, 9048–9058.
(7) Timkovich, R.; Cai, M. *Biochemistry* **1993**, *32*, 11516–11523.
(8) Turner, D. L.; Williams, R. J. P. *Eur. J. Biochem.* **1993**, *211*, 555–562.
(9) Bosshard, H. R.; Anni, H.; Yonetani, T. In *Peroxidases in Chemistry and Biology*; Everse, J., Everse, K. E., Grisham, M. B., Eds.; CRC Press: Boca Raton, FL, 1991; p 84.
(10) Kirk, T. K.; Farrell, R. L. *Annu. Rev. Microbiol.* **1987**, *41*, 465–505.
(11) Tien, M. *CRC Crit. Rev. Biochem.* **1987**, *15*, 141–168.
(12) Dunford, H. B. *Adv. Inorg. Biochem.* **1982**, *4*, 41.
(13) Poulos, T. L. *Adv. Inorg. Biochem.* **1988**, *7*, 1.
(14) Welinder, K. G. *Curr. Opin. Struct. Biol.* **1992**, *2*, 388–393.
(15) Yamada, H.; Makino, N.; Yamazaki, M. *Arch. Biochem. Biophys.* **1975**, *169*, 344–353.
(16) Makino, R.; Chiang, R.; Hager, L. P. *Biochemistry* **1976**, *15*, 4748–4754.
(17) Conroy, C. W.; Tyma, P.; Daum, P. H.; Erman, J. E. *Biochim. Biophys. Acta* **1978**, *537*, 62–69.
(18) Millis, C. D.; Cai, D.; Stankovic, M. T.; Tien, M. *Biochemistry* **1989**, *28*, 8484–8489.
(19) Banci, L.; Bertini, I.; Bini, T.; Tien, M.; Turano, P. *Biochemistry* **1993**, *32*, 5825–5831.
(20) Banci, L.; Bertini, I.; Turano, P.; Tien, M.; Kirk, T. K. *Proc. Natl. Acad. Sci. U.S.A.* **1991**, *88*, 6956–6960.
(21) de Ropp, J. S; La Mar, G. N.; Wariishi, H.; Gold, M. H. *J. Biol. Chem.* **1991**, *266*, 15001–15008.
(22) Banci, L.; Bertini, I.; Kuan, I-C.; Tien, M.; Turano, P.; Vila, A. J. *Biochemistry* **1993**, *32*, 13483–13489.
(23) Thanabal, V.; de Ropp, J. S; La Mar, G. N. *J. Am. Chem. Soc.* **1987**, *109*, 265–272.
(24) Thanabal, V.; de Ropp, J. S; La Mar, G. N. *J. Am. Chem. Soc.* **1987**, *109*, 7516–7525.
(25) Thanabal, V.; de Ropp, J. S; La Mar, G. N. *J. Am. Chem. Soc.* **1988**, *110*, 3027–3035.
(26) Satterlee, J. D.; Erman, J. E.; La Mar, G. N.; Smith, K. M.; Langry, K. C. *J. Am. Chem. Soc.* **1983**, *105*, 2099–2104.
(27) Satterlee, J. D.; Erman, J. E. *Biochemistry* **1991**, *30*, 4398–4405.
(28) Satterlee, J. D.; Russell, D. J.; Erman, J. E. *Biochemistry* **1991**, *30*, 9072–9077.
(29) Banci, L.; Bertini, I.; Turano, P.; Ferrer, J. C.; Mauk, A. G. *Inorg. Chem.* **1991**, *30*, 4510–4516.

0002-7863/95/1517-8659$09.00/0

Chart 1

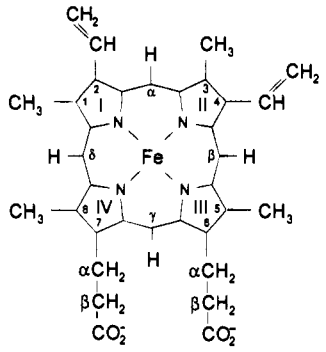

has been available for a long time,[31,32] and the X-ray structure of LiP has recently become available.[33-35] The crystallographic studies have confirmed many structural aspects ascertained from the NMR results. The latter investigation has also shown that the 2-vinyl group exhibits mobility,[22] and that its dominant solution orientation is different from that determined by the X-ray structure.[35]

All these peroxidases contain a pentacoordinated high-spin iron(III), with $S = 5/2$ in the resting state. The iron(III) is in the low-spin form with $S = 1/2$ state in their cyanide derivatives. The cyanide adduct is particularly well-suited for NMR investigations because the electron relaxation times of low-spin iron(III) may be very short (tending to 10^{-13} s). Furthermore, the effect of the unpaired electron on the relaxation of the nearby nuclei is relatively small.[36,37]

An extensive proton NMR assignment of a paramagnetic protein of molecular weight 40 000 is challenging as is characterizing the solution interaction of the enzyme with substrates and inhibitors. The available assignment of the ^{1}H NMR signals of the cyanide adduct of LiP (LiP−CN) is essentially limited to those signals which are shifted outside of the diamagnetic envelope.[20-22] Since the unpaired electron is located in the d_{xz} (or d_{yz}) orbital, as already discussed at length for many cyanide adducts of peroxidases and globins,[38-43] the signals experiencing sizable paramagnetic shifts are those located on the two opposite pyrroles. In LiP−CN, as well as in the cyanide adducts of several other peroxidases, these pyrroles are pyrroles II and IV (see Chart 1). This means that the proton signals of substituents in positions 3, 4, 7, and 8 experience large isotropic shifts and therefore are clearly detected outside of the diamagnetic envelope and can then be easily assigned. The assignment of signals which experience some coupling with the unpaired electron but fall in the diamagnetic envelope can also be achieved by using newly developed NMR methodologies. These methods have already been demonstrated to be useful for paramagnetic metalloproteins.[44-46] We have tested these techniques on the already thoroughly investigated HRP−CN protein.

We report here an extension of the assignment of the ^{1}H NMR spectrum of LiP−CN. This research is aimed at factoring the hyperfine shifts into their contact and pseudocontact contributions. If some protons experiencing pseudocontact shift are assigned, by referring to the available X-ray structure, it is possible to obtain information on the magnetic susceptibility anisotropy and on the direction of the χ tensor. It is then possible to determine the contact shift of the nuclei (protons, carbons, and nitrogens) which experience both contact and pseudocontact shift, allowing close insight into the electronic structure of the protein. Indeed, the extent of the magnetic susceptibility anisotropy is related to the extent of tetragonal and rhombic distortions; the contact shifts are related to the efficiency of the spin density transfer mechanism.

Studies on similar systems are available on metmyoglobin−CN (Mb−CN),[3] where a quite extensive NMR assignment is available,[47] and on HRP−CN,[48] where the structural data are still missing and reference was made to the CcP−CN structure.[32]

Finally, it is interesting to note that in LiP the orientation of the imidazole plane of the proximal histidine with respect to the heme plane, which largely defines the rhombicity of the system, is different from that of Mb[49,50] and is intermediate between the latter and that of CcP.[32]

Experimental Section

Sample Preparation. Horseradish peroxidase was obtained from Sigma Chemical Co. as a salt-free lyophilized powder (Sigma Type VI) and used without further purification. Lignin peroxidase from *P. chrysosporium* was prepared as previously reported.[51,52] All the NMR samples consisted of 0.5 mL of 2−3 mM protein sample in 100 mM phosphate buffer (pH 6.4−6.5) in D_2O solution.

NMR Spectroscopy. ^{1}H NMR spectra were recorded on a Bruker AMX 600 operating at 600.14 MHz. They were performed with the superWEFT[53] pulse sequence, using various recycle times, or by presaturating the solvent signal during the relaxation delay. The ^{1}H NOE experiments were performed with the superWEFT pulse sequence for water signal suppression and were collected using the previous reported methodology.[24,54] NOESY experiments[55] were recorded with presaturation of the residual solvent signal during both the relaxation delay (300−500 ms) and the mixing time (15−50 ms). They were

(30) Banci, L.; Bertini, I.; Pease, E. A.; Tien, M.; Turano, P. *Biochemistry* **1992**, *31*, 10009−10017.
(31) Poulos, T. L.; Kraut, J. *J. Biol. Chem.* **1980**, *255*, 8199−8205.
(32) Edwards, S. L.; Poulos, T. L. *J. Biol. Chem.* **1990**, *265*, 2588.
(33) Edwards, S. L.; Raag, R.; Wariishi, H.; Gold, M. H.; Poulos, T. L. *Proc. Natl. Acad. Sci. U.S.A.* **1993**, *90*, 750−754.
(34) Piontek, K.; Glumoff, T.; Winterhalter, K. *FEBS Lett.* **1993**, *315*, 119−124.
(35) Poulos, T. L.; Edwards, S. L.; Wariishi, H.; Gold, M. H. *J. Biol. Chem.* **1993**, *268*, 4429−4440.
(36) Bertini, I.; Luchinat, C. *NMR of paramagnetic molecules in biological systems*; Benjamin/Cummings: Menlo Park, CA, 1986.
(37) Banci, L.; Bertini, I.; Luchinat, C. *Nuclear and electron relaxation. The magnetic nucleus-unpaired electron coupling in solution*; VCH: Weinheim, 1991.
(38) Goff, H. M. In *Iron Porphyrins*; Lever, A. B. P., Gray, H. B., Eds.; Addison-Wesley: Reading, MA, 1983; pp 237−281.
(39) La Mar, G. N. In *Biological Applications of Magnetic Resonance*; Shulman, R. G., Ed.; Academic: New York, 1979; pp 305−343.
(40) Satterlee, J. D. In *Metal ions in biological systems*; Sigel, H., Ed.; Marcel Dekker: New York, 1987; pp 121−185.
(41) La Mar, G. N.; Walker, F. A. In *The Porphyrins*; Dolphin, D., Ed.; Academic Press: New York, 1979; pp. 61−157.
(42) Lee, K. -B.; La Mar, G. N.; Mansfield, K. E.; Smith, K. M.; Pochapsky, T. C.; Sligar, S. G. *Biochim. Biophys. Acta* **1993**, *1202*, 189−199.
(43) Bertini, I.; Turano, P.; Vila, A. J. *Chem. Rev.* **1993**, *93*, 2833−2932.
(44) Xavier, A. V.; Turner, D. L.; Santos, H. *Methods Enzymol.* **1993**, *227*, 1−16.
(45) *Biological Magnetic Resonance, Vol. 12: NMR of Paramagnetic Molecules*; Plenum Press: New York, 1993.
(46) Banci, L.; Bertini, I.; Luchinat, C. *Methods Enzymol.* **1994**, *273*.
(47) Emerson, S. D.; La Mar, G. N. *Biochemistry* **1990**, *29*, 1545−1556.
(48) La Mar, G. N.; Chen, Z. G.; Vyas, K.; McPherson, A. D. *J. Am. Chem. Soc.* **1995**, *117*, 411−419.
(49) Kuriyan, J.; Wilz, S.; Karplus, M.; Petsko, G. A. *J. Mol. Biol.* **1986**, *192*, 133−154.
(50) Cheng, X.; Schoenborn, B. P. *Acta Crystallogr. B* **1990**, *46*, 195.
(51) Tien, M.; Myer, S. B. *Appl. Environ. Microbiol.* **1990**, *56*, 2540−2544.
(52) Bonnarme, P.; Jeffries, T. W. *J. Ferment. Bioeng.* **1990**, *70*, 158−163.
(53) Inubushi, T.; Becker, E. D. *J. Magn. Reson.* **1983**, *51*, 128−133.
(54) Banci, L.; Bertini, I.; Luchinat, C.; Piccioli, M.; Scozzafava, A.; Turano, P. *Inorg. Chem.* **1989**, *28*, 4650−4656.
(55) Macura, S.; Wüthrich, K.; Ernst, R. R. *J. Magn. Reson.* **1982**, *47*, 351−357.

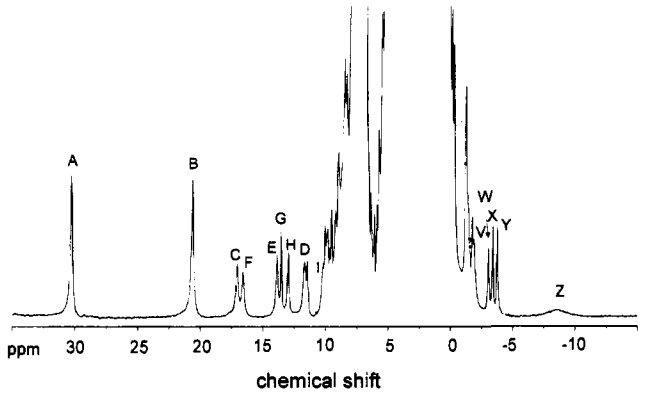

Figure 1. ^{1}H NMR (600 MHz) spectrum of LiP−CN recorded at 301 K, in 100 mM phosphate buffer at pH 6.4 in D_2O. The labeled signals were previously assigned (see Table 2).

collected using the TPPI method.[56] Arrays of 512−1024 FIDs of 1024−2048 data points were acquired. Sine-bell-squared weighting functions with 45−60° phase shifts were applied to the data. In a few cases, the NOESY sequence was preceded by a WEFT-type sequence (180° − τ),[57] using τ = 90 ms, to optimize the detection of signals due to fast-relaxing protons. NOE−NOESY experiments[58] with a mixing time of 50−100 ms were performed by using the conventional NOESY sequence, preceded by a selective irradiation (300 ms) of signals of interest. CLEAN−TOCSY experiments[59] were recorded with presaturation of the solvent signal and with a spin lock of 8−14 ms using the MLEV-17 pulse train.

Heteronuclear ^{1}H−^{13}C correlation spectra were recorded using a 5 mm inverse detection probe. The HMQC spectra consisted of 128−256 experiments acquired with 1024 data points each, in the magnitude mode, by using the standard pulse sequence[60,61] without decoupling during the acquisition time. A time of 2.5 ms was used as the refocusing delay.

To calculate the orientation of the magnetic anisotropy tensor χ, we have written a program[62] where we sampled all the possible orientations of the χ tensor (in steps of 5°) and, for each calculated orientation, looked for the best agreement of the calculated and experimental shifts by varying the χ tensor components. Once the first estimate of the best orientation was found, the calculations were repeated with finer angle variations around the first estimate values. By using the final χ tensor values and orientation, we have recalculated the pseudocontact shifts also for all the other protons not included in the minimization procedure.

Results

Heme Resonances. The ^{1}H NMR spectrum of LiP−CN recorded at 600 MHz in D_2O is shown in Figure 1. The labeled signals outside of the diamagnetic envelope have been previously assigned.[20−22] To extend the assignment of other heme protons of the heme, we performed ^{1}H−^{13}C HMQC experiments. Heteronuclear inverse-detection ^{1}H−^{13}C experiments have been successfully performed on paramagnetic low-spin heme proteins of lower molecular weight.[63−65] These experiments were developed after the pioneering work with direct detection.[66−68] We decided to record a ^{1}H−^{13}C HMQC spectrum of the cyanide adduct of HRP to test the feasibility of this kind of experiment on a 42 000 molecular weight paramagnetic protein. The refocusing delay in the pulse sequence was adjusted according to the T_2 values of the proton methyl signals and was set at 2.5 ms. A portion of the ^{1}H−^{13}C HMQC spectrum shown in Figure 2A reveals four well-defined cross peaks in the upfield ^{13}C region. These cross peaks correspond to the heme methyl groups. For HRP−CN, the ^{1}H NMR resonances for the four methyl signals have been already assigned through selective deuteration and saturation transfer experiments.[23] Two of the ^{1}H−^{13}C cross peaks, corresponding to the 8- and 3-CH_3 proton signals, fall outside of the proton diamagnetic envelope. The other two have a ^{1}H frequency corresponding to that of the 5- and 1-CH_3 signals.

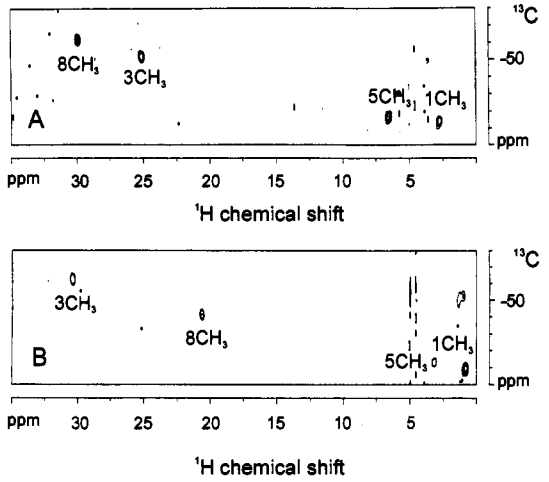

Figure 2. Portion of the ^{1}H−^{13}C HMQC spectrum of (A) HRP−CN and (B) LiP−CN. The spectrum in (A) was recorded at 310 K on a 3 mM sample of HRP−CN in 100 mM phosphate buffer at pH 6.5 in D_2O. Sample conditions for the spectrum in (B) are the same as those reported in Figure 1.

HMQC experiments have also been successfully performed on the cyanide adduct of LiP which has a molecular weight similar to that of HRP. A ^{1}H−^{13}C HMQC experiment performed on LiP−CN yielded the spectrum shown in Figure 2B. Four cross peaks which should correspond to the four methyl groups can be detected in the upfield carbon-shift region. This is the region where ^{13}C signals of the heme methyl groups in other low-spin iron(III) heme proteins are usually found.[63−65,69] Two of them have proton shift values which correspond to those of the most shifted 3-CH_3 and 8-CH_3 groups. The other two heme methyl groups are possibly detected at 3.3 and 0.8 ppm proton shifts and −11.7 and −8.4 ppm carbon shifts. Table 1 summarizes the carbon and proton shifts of the heme methyl groups of these peroxidases compared with those of Mb−CN.[64]

Once the two heme methyl proton resonances which fall in the diamagnetic region are located, we then attempt to discriminate between the 1- and the 5-CH_3 using WEFT−NOESY experiments.[70] In this experiment, a large part of the slow-relaxing signals are saturated, and therefore cross peaks between fast-relaxing signals, even if falling in the usual diamagnetic region, can be detected. In the experiment performed with a

(56) Marion, D.; Wüthrich, K. *Biochem. Biophys. Res. Commun.* **1983**, *113*, 967−974.
(57) Patt, S. L.; Sykes, B. D. *J. Chem. Phys.* **1972**, *56*, 3182.
(58) Bertini, I.; Dikiy, A.; Luchinat, C.; Piccioli, M.; Tarchi, D. *J. Magn. Reson., Ser. B* **1994**, *103*, 278−283.
(59) Griesinger, C.; Otting, G.; Wüthrich, K.; Ernst, R. R. *J. Am. Chem. Soc.* **1988**, *110*, 7870−7872.
(60) Bax, A.; Griffey, R. H.; Hawkins, B. L. *J. Magn. Reson.* **1983**, *55*, 301−315.
(61) Müller, L. *J. Am. Chem. Soc.* **1979**, *101*, 4481−4484.
(62) Banci, L.; Dugad, L. B.; La Mar, G. N.; Keating, K. A.; Luchinat, C.; Pierattelli, R. *Biophys. J.* **1992**, *63*, 530−543.
(63) Timkovich, R. *Inorg. Chem.* **1991**, *30*, 37−42.
(64) Banci, L.; Bertini, I.; Pierattelli, R.; Vila, A. J. *Inorg. Chem.* **1994**, *33*, 4338−4343.
(65) Turner, D. L.; Salgueiro, C. A.; Schenkels, P.; LeGall, J.; Xavier, A. V. *Biochim. Biophys. Acta* **1995**, *1246*, 24−28.
(66) Santos, H.; Turner, D. L. *FEBS Lett.* **1986**, *194*, 73−77.
(67) Yamamoto, Y. *FEBS Lett.* **1987**, *222*, 115−119.
(68) Yamamoto, Y.; Nanai, N.; Inoue, Y.; Chujo, R. *Biochem. Biophys. Res. Commun.* **1988**, *151*, 262−269.
(69) Santos, H.; Turner, D. L. *Eur. J. Biochem.* **1992**, *206*, 721−728.
(70) Chen, Z. G.; de Ropp, J. S.; Hernandez, G.; La Mar, G. N. *J. Am. Chem. Soc.* **1994**, *116*, 8772−8783.

Table 1. Proton and Carbon Shifts of the Heme Methyl Groups in the Cyanide Derivative of Some Heme Proteins As Measured from $^1H-^{13}C$ HMQC Experiments

	HRP−CN[a]		LiP−CN[b]		Mb−CN[c]	
signal	δ^1_H (ppm)	δ^{13}_C (ppm)	δ^1_H (ppm)	δ^{13}_C (ppm)	δ^1_H (ppm)	δ^{13}_C (ppm)
8-CH_3	28.7	−58.6	20.4	−39.8	12.5	−33.3
3-CH_3	24.9	−49.9	30.1	−60.0	4.9	−15.0
5-CH_3	6.6	−16.4	3.3	−11.7	26.4	−59.7
1-CH_3	2.8	−14.3	0.8	−8.4	18.2	−39.4

[a] Measured at 310 K. [b] Measured at 301 K. [c] Taken from ref 64, at 303 K.

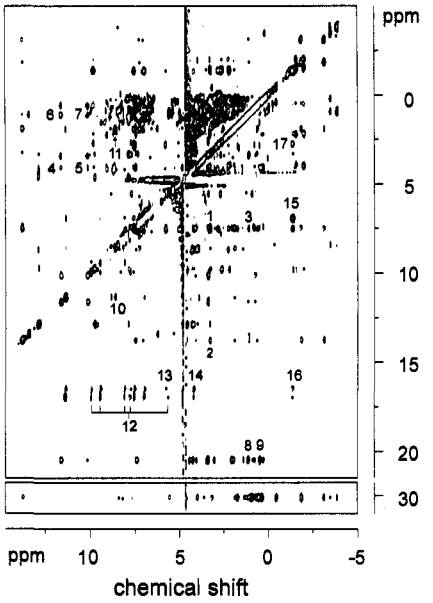

Figure 3. ^1H WEFT−NOESY (600 MHz) spectrum of LiP−CN, with a 50 ms mixing time. The recycle delay was 300 ms. Sample conditions are the same as those reported in Figure 1. Cross peak assignments: (1) Hβ-meso, 5-CH_3; (2) 4-Hα, 5-CH_3; (3) Hδ-meso, 1-CH_3; (4) 7-Hα, Hγ-meso; (5) 7-Hα', Hγ-meso; (6) 7-Hα, γ-CH_3 Val 184; (7) 7-Hα', γ-CH_3 Val 184; (8) 8-CH_3, γ-CH_3 Val 184; (9) 8-CH_3, δ-CH_3 Ile 235; (10) NHp His 176, NHp Ala 175; (11) NHp Ala 175, β-CH_3 Ala 175; (12) Hβs His 176, ring protons Phe 204 (see Figure 4); (13) Hβs His 176, Hβ Phe 193; (14) Hβs His 176, Hβ' Phe 193; (15) Hα His 176, Hα Ala 179; (16) Hβ2 His 176, β-CH_3 Ala 179; (17) Hα Ala 179, β-CH_3 Ala 179.

mixing time of 50 ms and a recycle time of 300 ms (Figure 3), two cross peaks between the CH_3 group at 3.3 ppm and a signal at 7.5 ppm (already assigned as Hβ-meso) (cross peak 1) and signal E at 13.8 ppm (already assigned as 4-Hα) (cross peak 2) are detected. We therefore assign the signal at 3.3 ppm as arising from the 5-CH_3 group. The fourth methyl signal at 0.8 ppm can be readily assigned as 1-CH_3. The WEFT−NOESY map shows the expected connectivities between the 1-CH_3 and the already assigned resonance of Hδ-meso at 7.4 ppm (cross peak 3) and between the 1-CH_3 and the 2-Hα at 8.4 ppm (this cross peak is observed with lower threshold). These results confirm the whole heme methyl proton assignment. Furthermore, a NOE−NOESY experiment[58] with saturation of the 8-CH_3 resonance has been performed. In this experiment, the NOESY spectrum of protons dipole−dipole connected with the irradiated one and those correlated to them through spin diffusion is selectively observed. The assignment of the 1-CH_3 is supported by the observed dipolar connectivities between the 8-CH_3 signal and the Hδ-meso proton and also between the latter and the 1-CH_3 signal, showing a magnetization transfer, 8-CH_3 → Hδ-meso → 1-CH_3 (data not shown). We have tested with success the feasibility of the detection of this pattern of

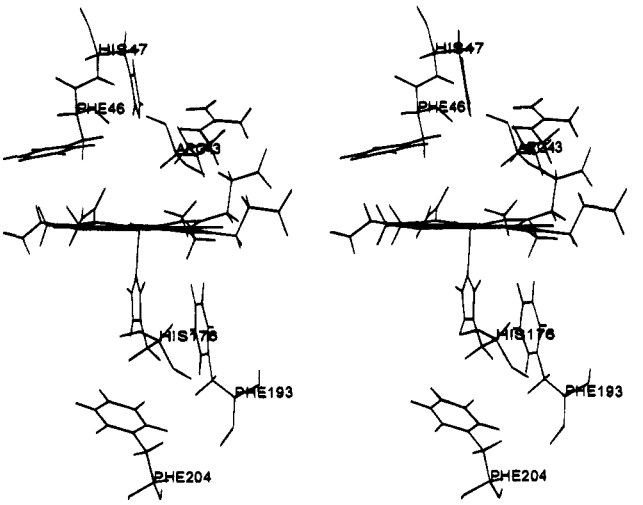

Figure 4. Stereoview of the active site of lignin peroxidase as derived from the X-ray structure.[35]

couplings among protons with interatomic distances and the relaxation parameters such as those of 8-CH_3, Hδ-meso, and 1-CH_3 by simulating the spectrum through the density matrix formalism.

Both of the resonances from the 7-Hα show a connectivity, in the WEFT−NOESY map (Figure 3) (cross peaks 4 and 5), with a signal at 4.1 ppm. The signal experiences a strong temperature dependence with negative slope and intercept at infinite temperature at about 11 ppm. Due to these features, we assign this signal as the Hγ-meso proton. With only the exception of the 6-propionate group the assignment of the proton signals of the heme ring is complete.

The 7-Hα protons are coupled with a resonance at 1.2 ppm (Figure 3, cross peaks 6 and 7), which experiences also a NOE with the 8-CH_3 (Figure 3, cross peak 8). Analysis of the X-ray structure[35] suggests that the signal at 1.2 ppm may correspond to the γ-CH_3 group of Val 184. This methyl group is the most likely candidate as it is the only group located close to the 7-Hα and 7-Hα' protons and to the 8-CH_3 group.

Proximal Side. The availability of the crystallographic structure of the enzyme has allowed the assignments of the ^1H NMR spectrum of LiP−CN to be extended to other residues in the proximal and distal sides (Figure 4).[35] Since the proton signals of the distal and proximal histidine residues (His 46 and 176, respectively) were unequivocally assigned,[21,22] we performed a series of NOE experiments by saturating their signals.

When signal Z (Hϵ_1 His 176) is saturated (data not shown), an intense NOE is detected with a signal at 0.3 ppm. Weaker NOEs are also found with the 1-CH_3 at 0.8 ppm, with the 8-CH_3 at 20.5 ppm, with the two Hβs of this histidine, and with a broad resonance at 7.6 ppm.

The projection of the proximal His plane is essentially oriented along pyrroles I and III in CcP while it is rotated toward the β/δ-meso protons in LiP, the Hϵ_1 proton pointing toward pyrrole I in both proteins. The angle between the projection on the heme plane of the His ring and the line connecting the δ- and β-meso carbons is about 8° in LiP, whereas it is about 30° in CcP. The observed NOEs with the heme methyl signals are consistent with the orientation of the proximal His in LiP in solution being similar to the one established by crystallography.[35] It has already been noted[20,22] that the small NOE detected in LiP−CN between the Hϵ_1 of His 176 and the 8-CH_3 group is not present in the cyanide adducts of CcP and HRP. This different behavior in different proteins of the same class in solution is in agreement with the crystallographic structures of LiP[35] and CcP.[31]

The signal at 0.3 ppm, coupled with Hϵ_1 of His 176, is also strongly dipole−dipole coupled with the 8-CH_3 resonance, as seen in the WEFT−NOESY map (Figure 3, cross peak 9). The signal at 0.3 ppm is relatively sharp, and its shift experiences a modest temperature dependence, indicating that the signal is due to a proton somewhat far from the metal ion. The only reasonable candidate for this intense NOE, consistent with its features and with the X-ray data,[35] is the δ-CH_3 of Ile 235, which is 2.9 Å from Hϵ1 of His 176 and which gives rise to a signal of intensity 3. We, therefore, tentatively assign the signal at 0.3 ppm as δ-CH_3 of Ile 235.

The signal at 7.6 ppm, which is dipole−dipole-coupled with Hϵ_1 of His 176, is broad, indicating that it should be close to the iron. Indeed, this signal has already been assigned as Hδ-meso.[20-22] The detection of a NOE between Hϵ_1 of His 176 and Hδ-meso is consistent with the structural arrangement of these protons (3.9 Å apart) (Figure 4). Another broad resonance is present, partially overlapping the signal at 7.6 ppm. A possible candidate for this resonance is Hζ of Phe 193 which is 4.6 Å from the iron and 3.3 Å from Hϵ_1 of His 176. However, no further evidence supports this assignment.

The signal at 11.4 ppm, which has been assigned as the peptidic NH of this histidine, is coupled (Figure 3, cross peak 10) with a signal at 8.6 ppm, whose shift experiences a very weak temperature dependence. This signal is strongly coupled with a signal at 1.9 ppm (cross peak 11), which also experiences a weak temperature dependence of the shift. From the behavior and the shift values of these signals, we assign the signal at 8.6 as the peptidic NH of Ala 175 and the signal at 1.9 ppm as the βCH_3 of the same residue.

The X-ray structure of LiP[35] shows that Phe 193 is located parallel to and close to His 176. Phe 204 is also placed near His 176, but with a different orientation and at a larger distance from the iron atom (Figure 4). Even if both Phe residues exhibited dipole−dipole connectivities with the proximal His, the different reciprocal orientations and the closer proximity of one of them to the iron atom would help us in differentiating their proton signals. Indeed, Phe 193 has the aromatic ring quite close to the iron. Consequently, its signals should be very broad and the complete pattern may not be observed. Phe 204 is expected to show the complete spin pattern since it is located farther from the paramagnetic center, and therefore its protons should give narrow signals. WEFT−NOESY experiments performed with short mixing time (50 ms) (Figure 3) show that the β-CH_2 protons of the proximal His are dipole−dipole-connected to several signals in the aromatic region (cross peaks 12). Five of them give well-defined NOESY (Figure 5A) and TOCSY (Figure 5B) patterns which correspond to a Phe residue. This pattern was already detected in a MCOSY map.[30] We assign these signals as belonging to Phe 204. Indeed, most of the aromatic ring protons of Phe 193 are far from the Hβs of His 176, and are not expected to give connectivities with them, with the exception of the Hδ_2. The assignment of Phe 204 is further supported by the observation that the signals experience relatively long relaxation times as it can be argued from the increased intensity of their cross peaks as the experimental recycle time is increased. The observed scalar connectivities (Figure 5B, cross peaks 1−4) allow us to pairwise assign the five ring proton resonances. Moreover, the relative intensities of their dipolar connectivities with the β-CH_2 protons of His 176 (Figure 3) allowed us to obtain a stereospecific assignment of these resonances (Table 2).

The Hβ protons of His 176 are coupled with two signals, at 5.8 and 4.2 ppm (Figure 3, cross peaks 13 and 14), which are also scalarly coupled (data not shown). The observed connectivities and the X-ray structure suggest that this proton pair arises from the Hβ protons of Phe 193. Furthermore, a signal at 7.5 ppm which experiences dipolar coupling with both of the Hβ protons of Phe 193 and with both of the Hβ protons of His 176 could be due to the Hδ_2 of Phe 193. The observed connectivities are consistent with the spatial disposition of these two residues. In such a way we have assigned all the connectivities involving the Hβ protons of His 176.

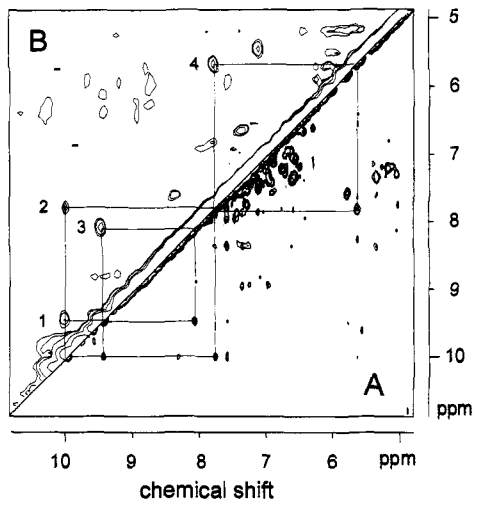

Figure 5. Section of the 600 MHz ^{1}H NOESY (A) and TOCSY (B) spectra of LiP−CN. Sample conditions are the same as those reported in Figure 1. Cross peak assignments: (1) Hζ Phe 204. Hϵ_1 Phe 204; (2) Hζ Phe 204. Hϵ_2 Phe 204; (3) Hϵ_1 Phe 204. Hδ_1 Phe 204; (4) Hϵ_2 Phe 204. Hδ_2 Phe 204.

A proton signal of intensity 3, which then should be due to a methyl group, is found in the upfield region at −1.4 ppm. This signal is strongly coupled with the Hα of His 176 (cross peak 15) and experiences dipolar coupling with the Hβ_2 of His 176 (cross peaks 16), as detected in the WEFT−NOESY experiment with a 50 ms mixing time (Figure 3). By looking at the X-ray structure, a good candidate is β-CH_3 of Ala 179. An intense NOESY connectivity between this methyl group resonance and a signal at 2.8 ppm can be attributed to the Hα protons of the latter residue (cross peak 17).

Distal Side. Two relevant residues are placed in the distal side in addition to the distal His (His 47): Phe 46 and Arg 43 (Figure 4). Arg 43 is conserved in all peroxidases whereas Phe 46 is present in all the proteins except the prokaryotic peroxidases.[14] Because they flank His 47, the dipolar connectivities from the protons of this His are essential in finding the signals of these residues. In this case, however, reference to the crystallographic data should be mentioned. It has been shown for the cyanide adduct of CcP that cyanide binding induces some rearrangements in the distal side affecting His 52, Trp 51, and Arg 48.[32] In LiP, the homologous residues are His 47, Phe 46, and Arg 43, respectively. Phe 46 is not involved in a hydrogen bond network as Trp 51 is in CcP; therefore, changes in the distal residue orientation should be small and only induced by steric hindrance. This conclusion is supported by the NOE network and by the experimental pseudocontact shifts (see later).

The assignment of protons of residues in the distal cavity has been obtained with the combined analysis of WEFT−NOESY, TOCSY, and NOE−NOESY experiments. The latter experiments are performed by saturation of the two nonexchangeable protons of the distal histidine. *i.e.*, Hδ_2 and Hϵ_1 of His 47 (signals H and G, respectively), and show several connectivities between these His protons and some other signals which are, in turn, coupled to each other.

Signal H experiences intense NOEs with a signal at 9.8 ppm

Table 2. Proton shifts (ppm) and Assignment of Signals in the Cyanide Adduct of LiP in D_2O, 100 mM Phosphate Buffer, pH 6.4. at 600 MHz

signal	δ (ppm)	assignment[e]	δ_{pc}^{calcd}	δ_{dia}[b]	δ_{cont}
		Heme Protons			
	0.8	1-CH_3	−5.8	3.9	2.7
	8.4	2-Hα[a]	−8.2	8.8	7.8
X	−3.5	2-$H\beta_{cis}$[a]	−3.8	6.4	−6.1
Y	−3.8	2-$H\beta_{trans}$[a]	−4.9	6.7	−5.6
A	30.1	3-CH_3[a]	−3.3	2.9	30.5
E	13.8	4-Hα[a]	−0.2	8.7	5.3
V	−1.8	4-$H\beta_{trans}$[a]	−0.8	6.6	−7.6
W	−3.1	4-$H\beta_{cis}$[a]	−0.6	6.9	−9.4
	3.3	5-CH_3	−6.0	3.8	5.5
D	11.6	7-Hα[a]	−4.6	4.9	11.3
I	10.1	7-Hα′[a]	−2.0	4.9	7.2
	3.4	7-Hβ[a]	0.1	3.9	−0.6
	0.9	7-Hβ′[a]	−0.8	3.9	−2.2
B	20.5	8-CH_3[a]	−1.1	3.9	17.7
	1.1	Hα-meso[a]	−15.1	9.8	6.4
	7.5	Hβ-meso[a]	−7.1	10.6	4.0
	4.1	Hγ-meso	−14.6	10.7	8.0
	7.4	Hδ-meso[a]	−6.8	10.7	3.5
		Proximal Side			
	1.9	β-CH_3 Ala 175	−0.5	1.8	
	8.6	NHp Ala 175	1.1	7.6	
	7.0	Hα His 176*,[a]	4.5	2.1	
C	17.0	$H\beta_1$ His 176[a]	7.2	−0.1	9.9
F	16.5	$H\beta_2$ His 176a	7.0	−0.9	10.4
Z	−8.4	$H\epsilon_1$ His 176[a]	23.8	2.0	−34.2
	14.0	$H\delta_1$ His 176[a]	13.0	9 to 11	−8 to −10
	13.3	$H\delta_2$ His 176[a]	22.4	1.4	−10.5
d	11.4	NHp His 176*,[a]	5.1	6.2	
	2.8	Hα Ala 179	−2.7	4.3	
	−1.4	β-CH_3 Ala 179*	−2.6	1.3	
	1.2	γ-CH_3 Val 184	−2.0	1.2	
	5.8	Hβ Phe 193	1.7 (2.6)	2.5 (2.4)	
	4.2	Hβ′ Phe 193	2.6 (1.7)	2.4 (2.5)	
	7.5	$H\delta_2$ Phe 193	1.3. 2.4	6.4	
	10.0	Hζ Phe 204*	3.7	6.7	
	9.5	$H\epsilon_1$ Phe 204*	3.5	6.7	
	8.1	$H\delta_1$ Phe 204*	2.1	6.7	
	7.8	$H\epsilon_2$ Phe 204*	2.3	5.9	
	5.7	$H\delta_2$ Phe 204*	1.7	4.4	
	0.3	δ-CH_3 Ile 235*	0.4	0.1	
		Distal Side			
	3.3	Hα Arg 43	−0.1	3.6	
	−1.9	Hβ Arg 43	−0.6	1.5 (2.0)	
	−1.3	Hβ′ Arg 43	−4.6	2.0 (1.5)	
	4.3	$H\gamma_1$ Arg 43*	5.6	−0.3	
	8.7	$H\gamma_2$ Arg 43*	10.5	−2.6	
	2.2	Hδ Arg 43	0.6. −2.1	2.3	
	4.6	$H\beta_1$ Phe 46*	1.3	3.0	
	7.9	$H\beta_2$ Phe 46*	4.9	1.9	
	4.6	Hα His 47	2.5	3.3	
G	13.4	$H\epsilon_1$ His 47*,[a]	7.1	5.9	
	17.0[c]	$H\delta_1$ His 47[a]	3.5	9 to 11	
H	12.9	$H\delta_2$ His 47*,[a]	8.3	5.7	
a	35.2[c]	$H\epsilon_2$ His 47[a]	24.6	9 to 11	
	9.8	NHp His 47	3.0	7.4	
		Axial Cyanide ^{15}N Resonance			
	608	$C^{15}N$[d]	68.3		

[a] Previously assigned (see refs 20−22). [b] The diamagnetic values were determined using the random coil values corrected for the effect of the protein secondary structure effect[78] and ring current effect. For the heme protons the diamagnetic values were taken from ref 95. [c] These signals are deected in H_2O solutions. [d] Taken from ref 22. [e] The asterisks indicate resonances used in the minimum input data set for searching the magnetic anisotropy components.

and a signal at 4.6 ppm (Figure 6, cross peaks 21 and 22). These two signals are also coupled to each other (cross peak 23). We assign the signal at 9.8 ppm as the peptidic NH of the distal His, which is 2.2 Å from the $H\delta_2$, and that at 4.6 ppm as the

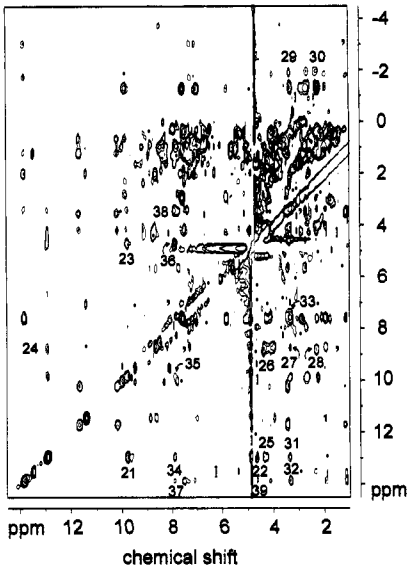

Figure 6. Expansion of the 600 MHz ^1H WEFT−NOESY spectrum of LiP−CN. with a 50 ms mixing time, reported in Figure 3. Cross peak assignments: (21) $H\delta_2$ His 47, NHp His 47: (22) $H\delta_2$ His 47, Hα His 47; (23) NHp His 47. Hα His 47: (24) $H\delta_2$ His 47, $H\gamma_2$ Arg 43; (25) $H\delta_2$ His 47, $H\gamma_1$ Arg 43; (26) $H\gamma_2$ Arg 43, $H\gamma_1$ Arg 43; (27) $H\gamma_2$ Arg 43. Hα Arg 43; (28) $H\gamma_2$ Arg 43, Hδ Arg 43; (29) Hα Arg 43, Hβs Arg 43 (30) Hδ Arg 43, Hβs Arg 43; (31) $H\delta_2$ His 47, Hα Arg 43; (32) 4-Hα, Hα Arg 43; (33) Hβ-meso. Hα Arg 43; (34) $H\delta_2$ His 47. $H\beta_2$ Phe 46; (35) NHp His 47. $H\beta_2$ Phe 46: (36) $H\beta_2$ Phe 46. $H\beta_1$ Phe 46; (37) 4-Hα, $H\beta_2$ Phe 46; (38) $H\beta_2$ Phe 46, Hα Arg 43: (39) 4-Hα, $H\beta_1$ Phe 46. The resonances of Hα Arg 43 and 5-CH_3 are coincident at 301 K.

Hα of the same residue, which is 3.6 Å from $H\delta_2$ and 2.9 Å from the peptidic NH. The presence of the latter signal in D_2O solutions could be due to the fact that this proton is buried in the protein. Indeed, also in HRP it has been found not to exchange with the bulk solvent.[70]

Signal H is also dipole−dipole coupled with a signal at 8.7 ppm and with a signal at 4.3 ppm (Figure 6, cross peaks 24 and 25). These two signals are coupled to each other, giving rise to a cross peak both in the NOESY (cross peak 26) and in the TOCSY (data not shown) maps. These two signals are broad, as can be estimated from the shape of the cross peak, and their shifts exhibit a strong temperature dependence, where their values decrease with an increase of temperature. These features suggest that these protons experience a large hyperfine coupling with the paramagnetic center. The signal at 8.7 ppm is also coupled, both in the NOESY and in the TOCSY maps, with two signals at 3.3 ppm (Figure 6, cross peak 27) and at 2.3 ppm (cross peak 28). The signal at 3.3 ppm is also dipolarly coupled with two upfield signals (at −1.9 and −1.3 ppm) (cross peaks 29) which are strongly coupled to each other, both dipolarly and scalarly. Also the signal at 2.3 ppm is dipole−dipole-coupled with the pair at −1.9/−1.3 ppm (cross peak 30). The pattern of connectivities, the presence of a scalar cross peak, and the properties of the signals suggest that the signal at 8.7 ppm is due to $H\gamma_2$ and that at 4.3 ppm to $H\gamma_1$ of Arg 43. The stereospecific assignment is supported by the relative intensities of the cross peaks with signal H. Furthermore, the signal at 4.3 ppm is coupled with the peptidic NH of His 47 as expected from the structure. We assign the signal at 3.3 ppm as Hα of this Arg. This assignment is further supported by the detection of dipolar connectivities with signal H (cross peak 31), with Hα of 4-vinyl (cross peak 32), and with Hβ-meso signals (cross peak 33), as expected from the X-ray structure. The signal at 2.3 ppm is assigned as Hδ of the same Arg, while the upfield pair is due to the Hβ protons of this distal Arg (Arg 43). The

other Hδ could possibly be the signal at 0.3 ppm which is dipolarly coupled with the signal at 2.3 ppm and the upfield pair at −1.9/−1.3 ppm. However, the lack of detection of any TOCSY cross peak involving this proton makes this assignment uncertain.

Finally, signal H experiences a strong NOESY cross peak with a signal at 7.9 ppm (Figure 6, cross peak 34). The latter signal is also coupled with the peptidic NH of the same histidine (cross peak 35) and is strongly coupled with a signal at 4.6 ppm (cross peak 36). We assign the signals at 7.9 and 4.6 ppm as due to the $H\beta_2$ and $H\beta_1$, respectively, of Phe 46. This assignment is further supported by the detection of NOESY connectivities between $H\beta_2$ of Phe 46 and Hα of 4-vinyl and Hα of Arg 43 (cross peaks 37 and 38) and between $H\beta_1$ of Phe 46 and Hα (cross peak 39) and $H\beta_{cis}$ of 4-vinyl (this cross peak is observed with lower threshold), as expected from the X-ray structure.

Signal G ($H\epsilon_1$ of His 47) experiences only a few connectivities with the proton falling in the diamagnetic region. In the NOE−NOESY map obtained by irradiating signal G, only a few resonances are observed. The more intense peak is at 6.3 ppm, and it has been hitherto detected in a MCOSY spectrum. It corresponds to a relaxation-allowed cross peak (*i.e.*, due to cross-correlation between proton-proton dipolar coupling and Curie-nuclear spin relaxation[71,72]), and it should therefore arise from a proton very close to the $H\epsilon_1$ of His 47. The nearest proton is $H\eta_{22}$ of Arg 43 which is located 2.2 Å from it. This strong NOE is present in D_2O solution, but it should be taken into account that the $H\eta_{22}$ is involved in a strong hydrogen bond network, according to the crystal structure. We do not have, however, any firm support for this hypothesis.

Factoring of the Hyperfine Shifts. Following the procedure outlined above, we have assigned several resonances of residues in the active site of LiP. Those protons which are several bonds away from the iron experience only pseudocontact contributions to the hyperfine shift. A best fitting of this contribution for several protons to the known dipolar shift equation can be attempted in order to determine the magnitude and the orientation of the magnetic anisotropy tensor, as done for other heme proteins[2−6,8] and metalloproteins.[62,73−76] By using the previously reported procedure,[62,73] we have sampled all the possible orientations of the χ tensor and, for each orientation, looked for the best agreement of the calculated and experimental shifts by varying the χ tensor components according to the following equation:[77]

$$\left(\frac{\Delta\nu}{\nu_0}\right)^{\text{pseudocont}} = \frac{1}{24\pi r^3}\{[2\chi_{zz} - (\chi_{xx} + \chi_{yy})](3\cos^2\theta - 1) + 3(\chi_{xx} - \chi_{yy})\sin^2\theta\cos 2\Omega\} \quad (1)$$

where χ_{kk} is the component of the magnetic susceptibility tensor along the three principal axes, θ is the angle between the z direction of the χ tensor and the proton−iron vector, and Ω is the angle between the projection of the proton−iron vector and the x axis.

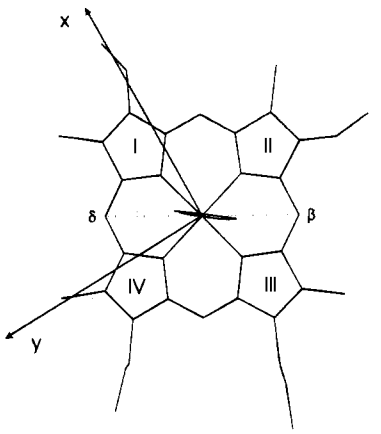

Figure 7. Schematic representation of the orientation of the magnetic anisotropy tensor in the frame of the heme moiety.

The axial and equatorial components of the magnetic susceptibily anisotropy are defined as

$$\Delta\chi_{ax} = \chi_{zz} - \frac{1}{2}(\chi_{xx} + \chi_{yy}) \quad \text{and} \quad \Delta\chi_{eq} = (\chi_{xx} - \chi_{yy})$$

The pseudocontact shifts are estimated from the observed shift values by subtracting the diamagnetic contribution. The latter has been evaluated from the shift values of protons of amino acids including protein secondary structure effects[78] and the ring current effects. These are computed using a program based on the Pullman approach[79] on the X-ray coordinates of LiP.[35]

By using the 15 resonances marked by an asterisk in Table 2 and which correspond to protons firmly assigned, values of 3.64×10^{-32} m^3 for $\Delta\chi_{ax}$ and of -1.51×10^{-32} m^3 for $\Delta\chi_{eq}$ are calculated. The z axis is tilted 1.2° from the perpendicular to the average plane passing through the four heme pyrrole nitrogens while the y axis makes an angle of −30° with the line connecting the δ- and β-meso carbons (Figure 7). These values for the magnetic anisotropy tensor come from the best fitting of the pseudocontact shifts to eq 1, assuming that the solution structure of the cyanide derivative is the same as that of the solid state cyanide-free protein. Comparison between the structures of CcP and CcP−CN[31,32] shows that the differences between the two structures are not very large. In any case, these differences are much smaller than those observed between the structures of CcP and LiP. At the moment the LiP X-ray structure is the best structural model available for the present calculations. Furthermore, the presence of a NOE between 8-CH_3 and $H\epsilon_1$ of the proximal histidine indicates that the orientation of the proximal histidine in solution is similar to that in the X-ray structure. Such a NOE is absent in both HRP−CN and CcP−CN.

When the fitting is performed over all the protons assigned in Table 2 except the heme and the proximal histidine protons, similar values for the magnetic anisotropies and orientations are found. Values of 3.76×10^{-32} m^3 for $\Delta\chi_{ax}$ and of -1.84×10^{-32} m^3 for $\Delta\chi_{eq}$ are obtained, with the z axis making an angle of 0.5° with the perpendicular to the heme plane and the y axis making an angle of −28.5° with the line connecting the δ- and β-meso carbons. This result is strong support for the assignments of the newly considered protons.

The direction of the z axis is consistent with expectations if the axial ligands are essentially perpendicular to the heme plane, as found in the X-ray structure of CcP−CN. An angle of 15°

(71) Bertini, I.; Luchinat, C.; Tarchi, D. *Chem. Phys. Lett.* **1993**, *203*, 445−449.
(72) Bertini, I.; Luchinat, C.; Piccioli, M.; Tarchi, D. *Concepts Magn. Reson.* **1994**, *6*, 307−335.
(73) Bertini, I.; Jonsson, B.-H.; Luchinat, C.; Pierattelli, R.; Vila, A. J. *J. Magn. Reson., Ser. B* **1994**, *104*, 230−239.
(74) Harper, L. V.; Amann, B. T.; Vinson, V. K.; Berg, J. M. *J. Am. Chem. Soc.* **1993**, *115*, 2577−2580.
(75) Shelling, J. G.; Bjorson, M. E.; Hodges, R. S.; Taneja, A. K.; Sykes, B. D. *J. Magn. Reson.* **1984**, *57*, 99−114.
(76) Capozzi, F.; Cremonini, M. A.; Luchinat, C.; Sola, M. *Magn. Reson. Chem.* **1993**, *31*, S118-S127.
(77) Kurland, R. J.; McGarvey, B. R. *J. Magn. Reson.* **1970**, *2*, 286−301.
(78) Wishart, D. S.; Sykes, B. D.; Richards, F. M. *J. Mol. Biol.* **1991**, *222*, 311−333.
(79) Giessner-Prettre, C.; Pullman, B. *Q. Rev. Biophys.* **1987**, *20*, 113−172.

Table 3. Factoring of the ^{13}C Contact Shifts for the Heme Methyl Groups in LiP-CN Using the Pseudocontact Shift Derived from the Magnetic Anisotropy Calculated in the Present Paper

LiP−CN methyl group	$^{13}C_{dia}$	$^{13}C_{pc}$	$^{13}C_{cont}$	$^{1}H_{cont}$[a]	$^{13}C/^{1}H$
8-CH_3	12.5	−1.3	−51.0	17.7	−2.9
3-CH_3	12.5	−3.8	−68.7	30.5	−2.2
5-CH_3	12.5	−7.2	−17.0	5.5	−3.1
1-CH_3	12.5	−7.0	−13.9	2.7	−5.1

was found in Mb−CN,[3] whereas for HRP−CN a quite large angle, 20°, was proposed.[48]

The y direction forms an angle of −38° with the projection of the axial ligand on the heme plane. In Mb−CN [3] and HRP−CN [48] the y axis coincides with the projection of the axial histidine. In general, the direction of the x and y magnetic axes in low symmetry systems depends both on the mixing of d_{xz} and d_{yz} orbitals *and* on the mixing of d_{z^2} and $d_{x^2-y^2}$, which are determined by the symmetry around the metal ion.[80,81]

Recently Turner[82] has elegantly shown how it is possible to determine the magnetic axes from the ^{13}C contact shifts, when the z molecular axis is perpendicular to the heme plane. However, the determination of such axes from first principles is a hard task. At this stage, we can only propose that the mixing of the z^2 orbital in the ground state is small because the magnetic z axis is perpendicular to the heme plane. The hyperfine shifts as such reflect bond strength as far as the contact contribution is concerned and both geometric distortions and bond strength as far as the pseudocontact contribution is concerned.

The knowledge of the magnetic anisotropy tensor allows us to factor the hyperfine shifts for all the nuclei for which they are available (Tables 2 and 3). The pseudocontact shifts are negative in the heme plane and are relatively small especially for the protons of groups linked to the pyrrole carbons.

The heme substituents, and particularly the methyl groups, experience a pairwise pattern for their contact shifts: the two opposite 8- and 3-CH_3 groups have large positive values while the other two opposite CH_3 experience negligible contact shift. The ^{1}H 3-CH_3 signal experiences the largest contact shift. This is qualitatively consistent with the predictions based on simple Hückel calculations.[83−85]

In Mb−CN the histidine plane lies along the line connecting pyrroles II and IV,[49,50] whose substituents are the ones experiencing the smallest contact shifts. In CcP−CN, the histidine plane lies along pyrroles I and III[31,32] and their substituents experience the smallest contact shifts. In the present case, the pattern of the contact shifts resembles that of CcP, although the plane of the proximal histidine is in a somewhat intermediate position between that of these two proteins.

The ^{13}C and ^{1}H contact shifts of the methyl groups experience a similar trend (Table 3), where the proton with the largest shift is attached to the carbon with the largest, in absolute value, shift. For the nuclei of the heme substituents, the contact contribution is determined by the unpaired spin density present on the heme pyrrole ring carbon to which the substituent is attached. As the origin of the unpaired spin density for the carbon and the proton of the heme substituents is the same, the ratio between the ^{13}C and the ^{1}H contact shifts for all the methyl groups should be the same. It has already been reported that this is the case for small symmetric complexes, whereas the ratio could be quite different in asymmetric proteins.[64,86] In the present system the variations are even larger (Table 3) than those previously reported. It should be noted, however, that the errors in proton contact shifts can be relatively large for 1- and 5-CH_3 which experience a small chemical shift.

It is worth noting that the shift of the Hϵ_2 (exchangeable, signal a) of the distal His can be reproduced very well with the calculated χ tensor (Table 2). This indicates that this proton in LiP is experiencing only dipolar coupling with the iron and no spin density is transferred through the H-bond with the CN^-. This is at variance with what is suggested for Mb−CN, where a contact contribution to the shift of the Hϵ_2 was proposed.[3,87]

The two nonexchangeable protons of the proximal His experience large negative contact shifts. The Hϵ_1 experiencies a much larger, in absolute value, contact shift than that observed for Mb−CN and larger than that of HRP−CN.

The axial magnetic anisotropy of LiP is slightly larger than that calculated for HRP−CN[48] (3.39×10^{-32} m^3)[96] (where it is assumed that the protein has the same structure as CcP−CN). The axial anisotropy for these two peroxidases is, however, smaller than that found for Mb−CN[3](4.18×10^{-32} m^3). It is interesting to note that the magnetic anisotropy of these systems parallels the anisotropy of the **g** tensor: larger anisotropies are found both for χ and for **g** for Mb−CN ($G_{ax} = 9.72$)[3,88,89] (where G_{ax} is defined as $[g_{zz}^2 - (1/2)(g_{xx}^2 + g_{yy}^2)]$) than for peroxidases (LiP, $G_{ax} = 7.44$; HRP, $G_{ax} = 6.38$[90]). The whole picture is consistent with a stronger axial bond in peroxidases than in globins and, between the peroxidases, a stronger axial bond in HRP than in LiP.

It has been suggested that the hyperfine shifts experienced by Hϵ_1 of the proximal histidine in various peroxidases and CcP mutants[20,91] and by the ^{15}N signal of cyanide[22] are related to the strength of the His−iron bond. This bond is believed to be very strong due also to a partial histidinato character of the proximal histidine[13,20,91,92] and to contribute to the negative Fe^{3+}/Fe^{2+} reduction potential in peroxidases. Now it appears that the hyperfine shift of the Hϵ_1 proton experiences a large pseudocontact contribution which is variable in the proteins analyzed here, whereas the contact term appears to be less variable. The large pseudocontact contribution is related to the extent of the axial magnetic anisotropy which on its turn may be related to the strength of the axial ligand. The stronger the ligand, the smaller the axial magnetic anistotropy. This anisotropy follows the order HRP−CN < LiP−CN < Mb−CN. So, the order of the Hϵ_1 hyperfine shifts may reflect the order of $\Delta\chi_{ax}$ and consequently the strength of the axial bond. Further studies on related systems, however, are needed before firm conclusions can be reached.

Concluding Remarks

In this work the heme methyl groups at positions 1 and 5 have been assigned. We have located some resonances of Arg 43, which is a conserved residue for all peroxidases and

(80) Gerloch, M.; Slade, R. C. *Ligand field parameters*: Cambridge University Press: Cambridge, 1973.
(81) Gerloch, M.; McMeeking, R. F. *J. Chem. Soc., Dalton Trans.* **1975**, 2443−2451.
(82) Turner, D. L. *Eur. J. Biochem.* **1995**, *227*, 829−837.
(83) Walker, F. A. *J. Am. Chem. Soc.* **1980**, *102*, 3254−3256.
(84) Walker, F. A.; Benson, M. *J. Phys. Chem.* **1982**, *86*, 3495−3499.
(85) Longuet-Higgins, H. C.; Rector, C. W.; Platt, J. R. *J. Chem. Phys.* **1950**, *18*, 1174−1181.
(86) Turner, D. L. *Eur. J. Biochem.* **1993**, *211*, 563−568.
(87) Lecomte, J. T. J.; La Mar, G. N. *J. Am. Chem. Soc.* **1987**, *109*, 7219−7220.
(88) Horrocks, W. DeW., Jr.; Greenberg, E. S. *Biochim. Biophys. Acta* **1973**, *322*, 38−44.
(89) Hori, H. *Biochim. Biophys. Acta* **1971**, *251*, 227−235.
(90) Blumberg, W. E.; Peisach, J.; Wittenberg, B. A; Wittenberg, J. B. *J. Biol. Chem.* **1968**, *243*, 1854.
(91) Satterlee, J. D.; Erman, J. E.; Mauro, J. M.; Kraut, J. *Biochemistry* **1990**, *29*, 8797−8804.
(92) Goodin, D. B.; McRee, D. E. *Biochemistry* **1993**, *32*, 3313−3324.

considered to be involved in a key step in the catalytic cycle.[93] We succeeded also in assigning some signals from two Phe residues in the proximal site and from one in the distal site, besides a few more protons (see Table 2). The hyperfine shifts experienced by residues not directly bound to the iron center are pseudocontact in origin. The pseudocontact shifts can be evaluated if the diamagnetic shifts are known, or as in the present case, they can be assumed within a reasonably small error by taking into account the possible sources of deviation from the random coil values.[94] From the pseudocontact shifts the anisotropy of the magnetic susceptibility tensor and its directions are determined. This allows us to factor the hyperfine shifts of the heme and proximal histidine protons into their contact and pseudocontact contributions. The magnetic susceptibility anisotropy tensor and the contact shifts are discussed in terms of the electronic structure of the metalloproteins as it depends on the symmetry and donor strength of the axial ligands. It appears that the axial anisotropy of the magnetic susceptibility tensor is larger in globins than in peroxidases, and larger in LiP than in HRP. This trend may be taken as the trend of the donor strength of the proximal histidine ligand.

A thorough analysis of the hyperfine shifts of the various nuclei in the NMR spectra may shed further light on the understanding of the electronic structure of peroxidases and globins.

Acknowledgment. The authors wish to thank Dr. David L. Turner for the useful discussions and for the use of his program to compute the ring-current shifts. Professor Gerd N. La Mar is gratefully acknowledged for making available his paper on the determination of the χ tensor in HRP−CN prior to publication.[48] R.P. acknowledges the Bruker Spectrospin Italiana s.r.l. for a postdoctoral fellowship. This research has been partially financed by the Progetto Strategico Tecnologie Innovative, Consiglio Nazionale delle Ricerche (CNR), EC Biotechnology Program No. BIO2-CT94-2052 (DG12SSMA), and U.S. Department of Energy Grant DE-FG02-87ER13690 to M.T.

JA950942H

(93) Vitello, L. B.; Erman, J. E.; Miller, M. A.; Wang, J.; Kraut, J. *Biochemistry* **1993**, *32*, 9807−9818.

(94) Wüthrich, K. *NMR of Proteins and Nucleic Acids*; Wiley: New York, 1986.

(95) Yamamoto, Y.; Nanai, N.; Inoue, Y.; Chujo, R. *Bull. Chem. Soc. Jpn.* **1988**, *62*, 1771−1776.

(96) These values have been recalculated by us from the original paper for comparison purposes.